

Novel Attenuated Total Reflection Fourier Transform Infrared Microscopy Using a Gem Quality Diamond as an Internal Reflection Element

SANONG EKGASIT* and PIMTHONG THONGNOPKUN

Sensor Research Unit, Department of Chemistry, Faculty of Science, Chulalongkorn University, Bangkok 10330, Thailand

A novel technique for attenuated total reflection Fourier transform infrared (ATR FT-IR) spectral acquisition by an infrared microscope with a gem-quality faceted diamond as an internal reflection element (IRE) is introduced. Unlike conventional IREs, the novel diamond IRE has a sharp tip configuration instead of a flat tip configuration. Light at normal incidence was coupled into the diamond while the transflected radiation from the diamond was collected through the table facet by the built-in 15× Cassegrainian objective. The number of reflections in the novel diamond IRE equals two. The evanescent field generated under total internal reflection at the pavilion facet was exploited for ATR spectral acquisition of materials attached to the IRE. The observed ATR spectra were compared to those obtained via a traditional zinc selenide IRE.

Index Headings: Faceted diamond; Attenuated total reflection; ATR spectrum; Fourier transform infrared; ATR FT-IR; Micro-ATR; Internal reflection element; Diamond IRE.

INTRODUCTION

Attenuated total reflection Fourier transform infrared (ATR FT-IR) spectroscopy is a molecular spectroscopic technique with unique surface-sensitive properties derived from the rapid decay of the strong evanescent field generated under the total internal reflection (TIR) phenomenon.¹⁻⁵ Although the rapid decay characteristic of the evanescent field makes the ATR spectrum sensitive to physicochemical phenomena near the interface, restrictions associated with the decay characteristic impose limitations on the application of the technique. The sample must optically contact the internal reflection element (IRE) in order to exploit the strong evanescent field near the interface. A small air gap can significantly deteriorate the observed spectra.⁶ In most cases, ATR spectra of a hard and rigid solid sample cannot be observed, even though the sample is mirror flat, due to insufficient contact. The ATR technique is most effective for the spectral acquisition of liquids, soft solids, or thin films that can be cast onto the IRE since optical contact can be easily achieved. In order to improve the contact of hard and rigid solid samples, force is applied onto the sample against the IRE.⁷⁻¹⁰ However, this operation must be performed with extreme care since the excessive force might damage the surface of the IRE. Another approach is to use an ATR accessory with an IRE with a small contact area in order to minimize the effect of local unevenness or roughness of the surface attached to the IRE.¹¹⁻¹³ There are numerous commercially available accessories designed for counteracting the contact problem. The hardest

rare type II natural diamond is employed in those accessories. Optical contact between the flat surface of the diamond IRE and a rigid solid sample can be easily achieved by simply pressing the two together.^{14,15}

This paper introduces a novel ATR FT-IR microscopy method using a gem-quality round brilliant cut diamond (~0.1 carat weight) as an IRE for spectral acquisition with an infrared microscope under the reflection mode. Unlike conventional IREs⁷⁻¹³ and commercially available diamond IREs,^{14,15} the novel approach employs a sharp-tip diamond IRE. The observed ATR spectra acquired with the diamond IRE will be compared to those acquired with a traditional zinc selenide (ZnSe) IRE.

THEORY

When electromagnetic radiation traveling within a denser medium (i.e., an IRE) impinges at the interface with a rarer medium of lower refractive index (i.e., a sample) at an angle of incidence greater than the critical angle, a strong evanescent field is generated at the interface. The evanescent field is strongest at the interface and decays exponentially as a function of the distance into the rarer medium. If the rarer medium is absorbing at the coupled frequency, the intensity of the reflected radiation becomes smaller than that of the incident radiation. The magnitude of reflection loss (or absorption) is proportional to the product between the imaginary part of the complex dielectric constant and the evanescent field amplitude. The absorbance $A(\theta, \nu)$ can be expressed in terms of the experimental conditions and material characteristics as:^{6,16}

$$A(\theta, \nu) = \frac{(2\pi\nu)^2}{\ln(10)k_{z,\text{IRE}}(\theta, \nu)} \cdot \frac{d_p(\theta, \nu)}{2} \times \text{Im}[\hat{\epsilon}_{\text{sample}}(\nu)] \langle E_0^2(\theta, \nu) \rangle \quad (1)$$

where θ is the angle of incidence, ν is the frequency of the incident radiation, $\hat{\epsilon}_{\text{sample}}(\nu)$ is the complex dielectric constant of the sample, $d_p(\theta, \nu)$ is the penetration depth, $\langle E_0^2(\theta, \nu) \rangle$ is the mean square evanescent field (MSEvF) at the IRE/sample interface, and $k_{z,\text{IRE}}(\theta, \nu)$ is the z -component wave-vector within the IRE. The wave-vector can be expressed in terms of the x -component wave-vector $k_{x,\text{IRE}}(\theta, \nu)$ by $k_{z,\text{IRE}}(\theta, \nu) = [(2\pi\nu)^2\epsilon_{\text{IRE}} - k_{x,\text{IRE}}(\theta, \nu)]^{1/2}$, where $k_{x,\text{IRE}}(\theta, \nu) = 2\pi[\epsilon_{\text{IRE}} \sin^2\theta]$ and ϵ_{IRE} is the dielectric constant of the prism. The detailed derivations of the MSEvF are given elsewhere.^{17,18} The penetration depth, defined as the distance at which the MSEvF decays to 1/e of that at the interface, is given in terms of experimental conditions and material characteristics by $d_p(\theta, \nu)$

Received 22 April 2005; accepted 6 July 2005.

* Author to whom correspondence should be sent. E-mail: sanong.e@chula.ac.th.

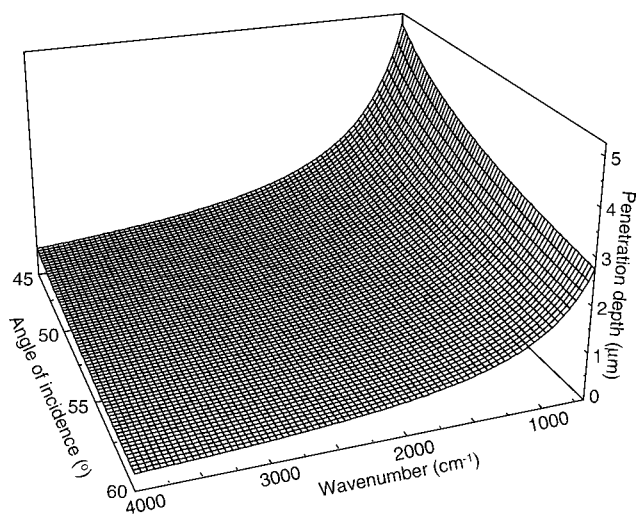


FIG. 1. Penetration depth in the mid-infrared region at various angles of incidence with a ZnSe IRE.

$= 1/[k_{x,IRE}(\theta, \nu) - (2\pi\nu)^2\epsilon_{IRE}]^{1/2}$. Although the penetration depth is not the actual distance from the interface where the evanescent field interacts with the sample, it is the figure that indicates relative depth-dependent information acquired under various experimental conditions. The actual distance at which the spectral information was acquired (i.e., the sampling depth) is greater than the penetration depth.¹⁹ The penetration depth profile in the mid-infrared region shown in Fig. 1 implies that absorption bands at various frequencies in an ATR spectrum do not provide information up to the same depth. The greater the frequency and/or the angle of incidence, the shallower is the depth of the acquired spectral information. An observed ATR spectrum is the collective molecular information from the IRE/sample interface up to the depth (i.e., sampling depth) at which the MSEvF decays to an insignificant level. The sampling depth in an ATR FT-IR spectrum is varied depending on the experimental conditions (i.e., angle of incidence and frequency of the coupled radiation) and material characteristics (i.e., refractive indices of the IRE and sample). In general, the value is approximately a few micrometers from the IRE/sample interface. However, it should be noted that the majority of the spectral information comes from chemical moieties near the interface, where the MSEvF is strongest. The spectral contribution at a greater depth decreases exponentially as the evanescent field decays.

Diamond can be employed as an IRE due to its high refractive index ($n_{\text{Diamond}} = 2.417$) and partial optical transparency in the mid-infrared region. Diamond has three major absorption bands in the mid-infrared region, namely one-phonon ($1400\text{--}900\text{ cm}^{-1}$), two-phonon ($2650\text{--}1500\text{ cm}^{-1}$), and three-phonon ($3900\text{--}2650\text{ cm}^{-1}$) absorptions.²⁰ The absorption magnitude in the one-phonon region depends strongly on the concentration of nitrogen impurities. Diamond with a high nitrogen content always shows over-absorption in this region.²¹ Although the two-phonon region is always over-absorbing, it has little effect on the analysis of organic materials since most of the materials do not absorb in this region. The three-phonon absorption, on the other hand, is very weak. It imposes insignificant interference on the absorption of

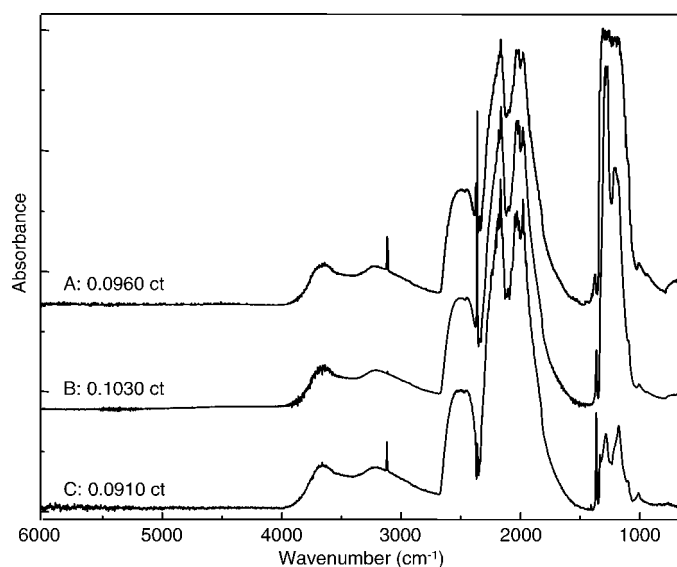


FIG. 2. Transmittance spectra of round brilliant cut natural diamonds with different levels of nitrogen impurities: (A) 0.0960 ct, (B) 0.1030 ct type IaA, and (C) 0.0910 ct type IaB. An absorption band at 2350 cm^{-1} is due to a fluctuation of atmospheric carbon dioxide during the spectral acquisition.

the materials. Transmittance spectra of round brilliant cut diamonds with different magnitudes of nitrogen and hydrogen impurities are shown in Fig. 2. Absorption bands associated with impurities are clearly observed. The observed spectral envelopes in the one-phonon region indicate that the diamonds are of different types. The diamonds in Figs. 2B and 2C are of type IaA and IaB, respectively, while that in Fig. 2A cannot be identified due to the over-absorption in the one-phonon region. A sharp peak at 3107 cm^{-1} is assigned to the vinylidene vibration of the hydrogen impurities in the diamond crystal structure. The intensity of the peak varies considerably with the concentration of hydrogen impurity in the diamond crystal structure.^{20,21}

In principle, a faceted diamond is cut in such a proportion that the number of total internal reflections within the diamond is enhanced. To increase the number of total internal reflections, the cutting proportion of the diamond is carefully designed with respect to its refractive index, size, shape, and carat weight. The number of reflections depends on the angle and positions at which light enters the diamond. The greater the number of total internal reflections, the better is the fire and brilliance of the diamond. This phenomenon is due to the dispersion of light associated with its traveling distance and the total internal reflection inside the diamond.^{22,23} A schematic illustration of ray tracings within a round brilliant cut diamond is shown in Fig. 3. In order to collect transmittance spectra of a faceted diamond using an infrared microscope, the infrared radiation is coupled into and is collected from the table facet by the built-in $15\times$ Cassegrainian objective.²⁴ For the coupled radiation with a normal incidence to the table facet, the radiation totally reflects at the pavilion facet. Under the employed cut proportion (i.e., a set of Tolkowsky's recommended proportion with pavilion angle of 41° and crown angle of 34°),^{20,21} the angles of reflection at the pavilion facet are 41° and 57° for the first and second reflections, respectively. The radiation

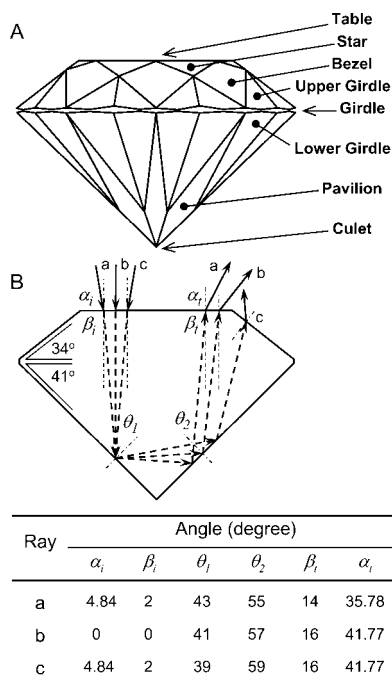


FIG. 3. (A) A schematic illustration of a round brilliant cut diamond with Tolkowsky's recommended proportion. (B) Ray tracing of the coupled radiations within the faceted diamond. Angles of reflection and refractions defined with respect to the direction normal to the reflecting surfaces are summarized.

reaches the diamond/air interface at the table facet with an angle of 16° and refracts into air with an angle of 41.77° . Due to the complex cut surfaces of the faceted diamond, the coupled radiations that impinge the table facet with different angles and/or positions undergo different reflections inside the faceted diamond before emerging into air at any facet. According to the traveling path of the coupled radiation, the outgoing radiation from the table facet is defined as the *transflected radiation*. The evanescent field generated under total internal reflection at the pavilion facets can interact with a material attached to the diamond. By collecting the transreflectance spectrum, absorption of the material under ATR conditions can be observed.

EXPERIMENTAL

All FT-IR spectra were collected using a Nicolet Magna 750 FT-IR spectrometer equipped with a mercury-cadmium-telluride (MCT) detector. Spectra in the mid-infrared region ($4000\text{--}650\text{ cm}^{-1}$, unless otherwise specified) with a spectral resolution of 4 cm^{-1} with 512 coadded scans were employed. A commercial single-reflection ATR accessory (The Seagull™, Harrick Scientific) with a 25 mm hemispherical ZnSe IRE was employed for all conventional ATR FT-IR spectral acquisitions. For the novel ATR FT-IR spectral acquisition using an infrared microscope, a gem-quality round brilliant cut natural diamond type IaB (0.0910 carat) was employed as an IRE. The defect-free diamond was mounted onto a homemade micro-ATR accessory. The homemade accessory has a sample holder whereby a solid sample can be brought into contact with the culet of the diamond IRE. Infrared radiation from the infrared microscope (Model NIC-

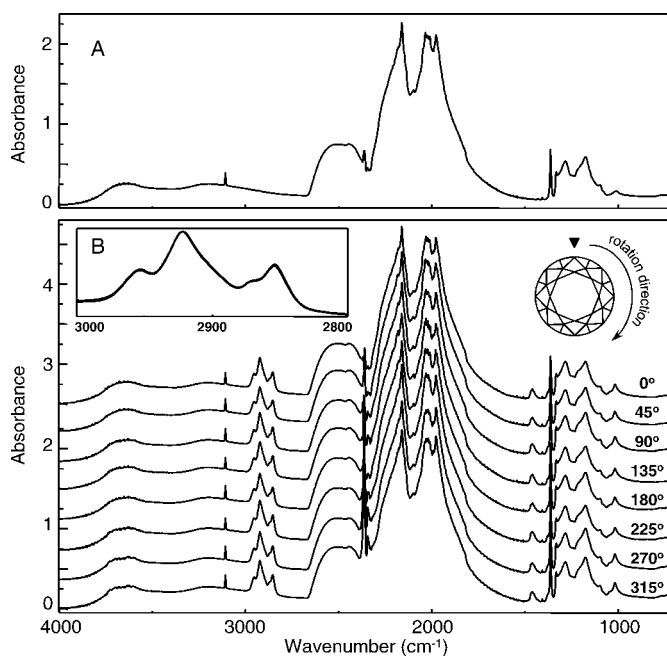


FIG. 4. (A) Transflectance spectra of the employed diamond IRE (0.0910 ct type IaB). (B) ATR spectra of a minute amount of mineral oil on the culet of the diamond IRE with different angles of diamond rotation. The inset shows the superimposition of the ATR spectra of the mineral oil in the CH stretching region.

PLAN, Nicolet) attached to the FT-IR spectrometer was coupled into the diamond while the transreflectance radiation was collected via the built-in $15\times$ Cassegrainian objective through the table facet. Reflection with normal incidence from a gold mirror was employed as a background for all ATR FT-IR spectra acquired by the microscope.

As shown in Fig. 3, unlike conventional IREs^{7–13} and commercially available diamond IREs,^{14,15} the sampling area of the novel IRE is the sharp pavilion facet of the cut and polished diamond. The effective number of reflections equals two. Due to the divergent nature of the focusing optics, although the radiation was coupled under normal incidence to the table facet, the angle of incidence at the diamond/sample interface was not well defined but instead covered a range of angles. As a result, the observed spectrum is the collective spectral information of all possible angles.

RESULTS

Transflectance spectra of the employed diamond IRE (i.e., ATR spectra of air) are shown in Fig. 4A. Since diamond is absorbing in the mid-infrared region, absorptions at the characteristic frequencies of diamond are expected when it is employed as an IRE for ATR measurements. The three fundamental absorption bands and the absorption bands associated with nitrogen and hydrogen impurities in the diamond crystal structure were clearly observed. The employed diamond IRE is classified as a type IaB diamond based on the spectral envelope in the one-phonon region. Since the bands are unique to diamond, they appear in all ATR FT-IR spectra acquired with the diamond IRE with a specular reflection from a gold mirror as a reference. ATR spectra of a minute

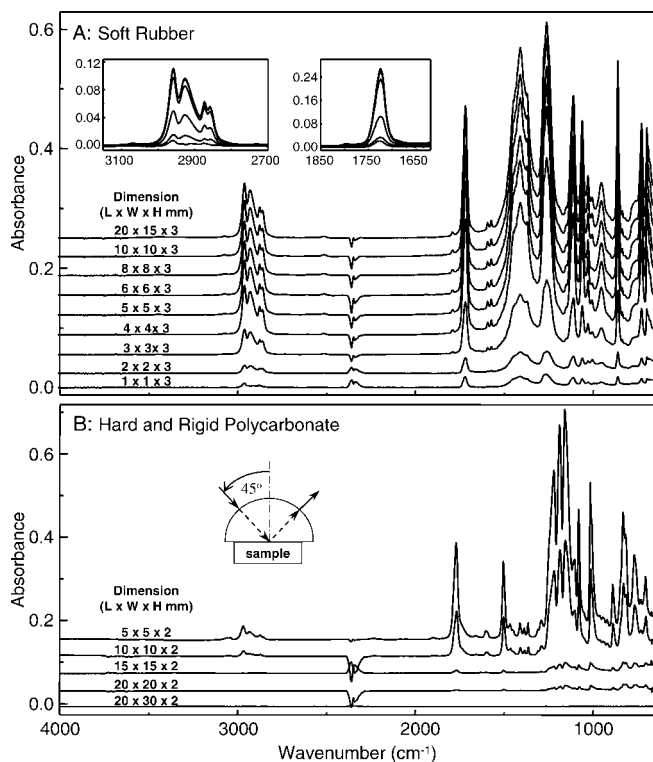


FIG. 5. (A) ATR spectra of soft rubbers of different sizes. The observed spectra do not change when the size is greater than 5×5 mm. (B) ATR spectra of mirror-flat polycarbonate specimens of different sizes. The specimens were pressed against the hemispherical ZnSe IRE. The shown spectra were those with unchanged absorption as the pressure was increased.

amount of mineral oil deposited on the culet are shown in Fig. 4B. The mineral oil covers the culet and a very small portion of the pavilion facet near the culet. When the diamond IRE was rotated to different angles with respect to a reference position, the observed spectra were superimposed. Although there are some negligible discrepancies among the observed spectra due to minor variations associated with the diamond alignment, Fig. 4B indicates that it does not have any influence on the observed ATR spectra.

Spectra in Fig. 5A show the influence of sample size on the absorption magnitude. According to the optical design of the employed single-reflection ATR accessory, the illumination area on the surface of the hemispherical IRE is relatively small compared to the flat surface of the IRE. The experimental results indicate that the illumination area is approximately 25π mm² at the center. When optical contact is achieved (i.e., with a soft solid or liquid), further increments of the sample size larger than the illumination area do not increase the absorption. The influence of sample contact is shown in Fig. 5B. ATR spectra of hard and rigid solid polycarbonate with mirror-flat surfaces indicate that the small specimen ($5 \times 5 \times 2$ mm) possesses a much greater absorption magnitude compared to those of the large specimens. This is due to the insufficient contact between the large polycarbonate sample and the IRE compared to that of the small one. Good contact for a small sample can be achieved by simply applying pressure on the sample against the IRE.^{7-9,14,15} A large specimen tends to have a surface with

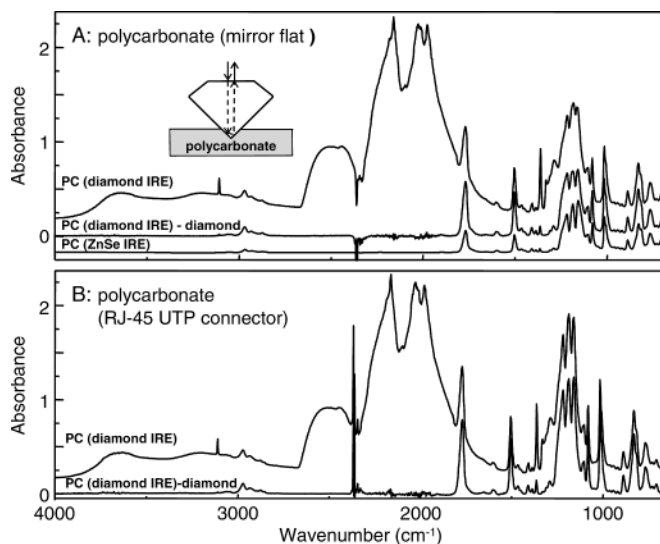


FIG. 6. (A) ATR spectra of a mirror-flat polycarbonate acquired using the novel diamond IRE. The specimen is the same as that in Fig. 5B. (B) ATR spectra of a complex-shaped polycarbonate (an RJ-45 UTP connector for the Ethernet card). When the contributions of the diamond IRE were subtracted, the unique spectral features of the polycarbonate were revealed. An ATR spectrum of polycarbonate acquired using the ZnSe IRE is overlaid for comparison.

local unevenness or a surface with small particles that prevent good contact. As a result, the observed ATR spectrum becomes deteriorated. In the worst case, an ATR spectrum of a hard and rigid solid sample cannot be observed at all.⁶

An ATR spectrum of the same specimen acquired with the diamond IRE, on the other hand, does not suffer from the variation of the sample size since the sampling area is governed by the small contact area of the diamond IRE (see Fig. 6A). The diamond tip (i.e., the culet and part of the pavilion facet) is utilized as the sampling area where the evanescent field interacts with the sample. The contact area between the diamond IRE and sample can be manipulated via the penetration of the diamond tip into the sample. Since the diamond tip is very small, the problems associated with the contact were eliminated while the diamond tip always possesses good contact with the hard and rigid solid sample. Pressure can be applied onto the sample against the diamond IRE to ensure optimal contact during spectral acquisition. ATR spectra of the hard and rigid polycarbonate with complex shapes (RJ-45 UTP connector for Ethernet card) are shown in Fig. 6. Due to the small contact area of the diamond IRE, the observed ATR spectrum was not affected by the surface irregularity or roughness of the specimen. It should be noted that ATR spectra of such specimen cannot be observed by the conventional ATR technique without additional sample preparation. For the current spectral acquisition with the novel diamond IRE, the specimen was simply brought into contact with the IRE and the ATR spectrum was taken. When the absorption of diamond was subtracted from the observed spectra, unique spectral features of the polycarbonates were revealed. However, the contribution of the diamond absorption cannot be completely eliminated due to the differences in the optical configurations of the systems (i.e., diamond/air and diamond/polycarbonate). Although the

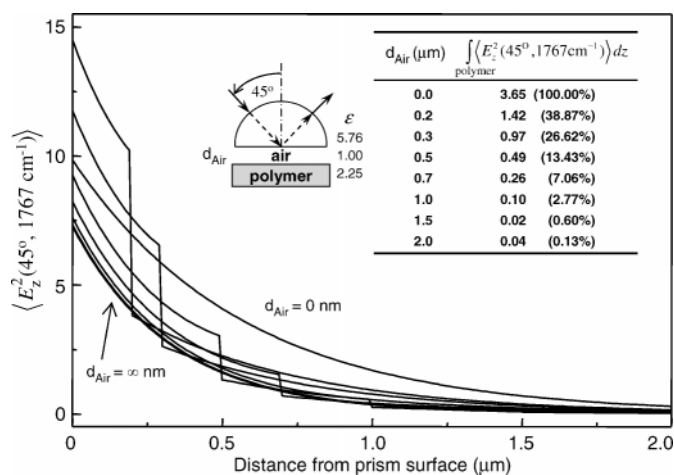


FIG. 7. The MSEvF with different thicknesses of air gaps. The MSEvF integration within the polymer layer (inserted table) decreases significantly as the thickness of the air gap increases. The simulation parameters are shown.

absorption of diamond in the two-phonon region was completely subtracted, absorption of diamond at 3107 cm^{-1} is still observable. As a result, absorption of diamond in the one-phonon region was still present in the subtracted spectra. Due to strong absorption of the polycarbonate in the region, residual absorption of the diamond in the one-phonon region was obscured.

DISCUSSION

The ability of the ATR technique to selectively acquire molecular information within the region up to few micrometers from the surface is derived from the unique properties of the evanescent field generated under total internal reflection. According to Eq. 1 and the frequency-dependent nature of the penetration depth, the absorption in an ATR spectrum is strongly dependent on the degree of contact between the IRE and the sample. If good contact is not achieved, integration of the MSEvF within the sample (thus, the absorbance) becomes smaller (see Fig. 7). When good contact is not achieved in the IRE/polymer two-phase system, an air gap exists between the IRE and the polymer. The system becomes a three-phase system (i.e., IRE/air/polymer). The integration of the evanescent field within the polymer is drastically decreased as the thickness of the air gap increases. Although there is a field enhancement within the air gap due to optical effects, the field does not contribute to the absorption of the polymer. Under the conditions defined in Fig. 7, when the thickness of the air gap is greater than $1.00\text{ }\mu\text{m}$, the field integration within the polymer becomes insignificantly small compared to that without an air gap. As a result, the absorption of the polymer at the defined frequency cannot be observed. As shown in Fig. 5B, for a hard and rigid solid sample absorption of the small sample with better contact is greater than that of the big sample with poor contact. Since good contact is necessary for the measurement of a good-quality ATR FT-IR spectrum, a small sample or an IRE with a small contact area was employed for contact improvement.^{14,15} Since the employed commercial ATR accessory has focusing optics with a small illumination area on the flat surface of the

hemispherical IRE, it is suitable for spectral acquisition of a small, hard and rigid solid sample with a mirror-flat surface. However, for a solid sample with a rough and curved surface or that with a complex shape, good contact with the IRE is not normally achieved while the observed ATR spectrum is deteriorated.

The small diamond IRE eliminates problems associated with sample contact. It can be employed for ATR spectral acquisitions of hard and rigid solid materials that cannot normally be measured by conventional ATR accessories. Since diamond is the hardest known material, it cannot be easily damaged by an excessive force under normal operations. Good contact is always achieved by simply pressing the sample against the diamond IRE. No sample preparation or minimal sample preparation is required when collecting spectra using the novel diamond IRE. Since diamond is an isotropic medium while the coupled radiation from the Cassegrainian objective is non-polarized,²⁴ rotation of the diamond IRE does not introduce any change in the absorption of diamond. However, a negligible discrepancy between consecutive measurements may be observed since the exact degree of perpendicularity between the coupled radiation and the table facet cannot be re-created. One major drawback of the diamond IRE is its inherent strong absorption in the one-phonon regions. Absorption of the sample in these regions will be masked by the diamond absorptions. However, this problem can be eliminated by employing a synthetic diamond or a type II natural diamond with extremely low nitrogen content.

CONCLUSION

A novel ATR FT-IR spectral acquisition method using an infrared microscope with a gem-quality faceted diamond as IRE was developed. The small diamond tip eliminates the problems associated with an air gap or insufficient contact between the solid sample and the IRE. The hard and rigid solid sample with a rough surface can be brought into contact with the diamond IRE while pressure can be applied in order to ensure optimal contact during measurement. Since diamond is the hardest known material, ATR FT-IR spectra of hard and rigid solid materials can be measured (especially those with rough surfaces or irregular shape). One of the major drawbacks of the employed type IaB natural diamond IRE is the masking absorption bands in the one-phonon region. However, the problem can be overcome by employing a diamond with low levels of nitrogen impurity or a rare type II natural diamond with extremely low nitrogen impurity.

ACKNOWLEDGMENTS

The authors gratefully acknowledge support from Chulalongkorn University through University Research Unit and the Ratchadaphisek Somphot Endowment, partial funding from the National Research Council of Thailand (NRCT) through the Nanopolymer Project (contract number GOR-SOR-SOR 52/2547), and an instrumental donation from Seagate Technology Co. Ltd. (Thailand). A fellowship for P.T. from the University Development Committee (UDC) is gratefully acknowledged.

1. N. J. Harrick, *Internal Reflection Spectroscopy* (Harrick Scientific Corporation, Ossining, New York, 1987).
2. V. Koppaka and P. Axelsen, *Langmuir* **17**, 6309 (2001).

3. M. W. Urban, *Attenuated Total Reflection Spectroscopy of Polymers* (American Chemical Society, Washington, D.C., 1996).
4. A. S. Cantor, *J. Control. Release* **61**, 219 (1999).
5. E. Goormaghtigh, V. Raussens, and J.-M. Ruysschaert, *Biochim. Biophys. Acta* **1422**, 105 (1999).
6. S. Ekgasit, *Appl. Spectrosc.* **54**, 756 (2000).
7. T. Buffeteau, B. Desbat, and D. Eyquem, *Vib. Spectrosc.* **11**, 29 (1996).
8. G. Muller and C. Riedel, *Fresenius' J. Anal. Chem.* **365**, 43 (1999).
9. C. M. Balik and W. H. Simendinger, *Polymer* **39**, 4723 (1998).
10. V. Acha, M. Meurens, H. Naveau, and S. N. Agathos, *Biotech. Bioeng.* **68**, 473 (2000).
11. A. J. Sommer and M. Hardgrove, *Vib. Spectrosc.* **24**, 93 (2000).
12. D. J. Lyman, J. Murray-Wijelath, and M. Feughelman, *Appl. Spectrosc.* **55**, 552 (2001).
13. D. J. Lyman and J. Murray-Wijelath, *Appl. Spectrosc.* **59**, 26 (2005).
14. A. M. Young, *Biomaterials* **23**, 3289 (2002).
15. A. M. Young, S. A. Rafeeka, and J. A. Howlett, *Biomaterials* **25**, 823 (2004).
16. S. Ekgasit and A. Padermshoke, *Appl. Spectrosc.* **55**, 1352 (2001).
17. W. N. Hansen, *J. Opt. Soc. Am.* **58**, 380 (1968).
18. W. N. Hansen, "Internal Reflection Spectroscopy," in *Advances in Electrochemistry and Electrochemical Engineering*, R. H. Muller, Ed. (John Wiley and Sons, New York, 1973), vol. 9.
19. F. M. Mirabella, Jr., *J. Polym. Sci. Polym. Phys. Ed.* **21**, 2403 (1983).
20. M. J. Mendelssohn and H. J. Milledge, *Int. Geol. Rev.* **37**, 95 (1995).
21. W. Wang, T. Moses, R. C. Linares, J. E. Shigley, M. Hall, and J. E. Butler, *Gem. Gemology* **39**, 268 (2003).
22. T. C. Hemphill, I. M. Reinitz, M. L. Johnson, and J. E. Shigley, *Gem. Gemology* **34**, 158 (1998).
23. I. M. Reinitz, M. L. Johnson, T. C. Hemphill, A. M. Gilbertson, R. H. Geurts, B. D. Green, and J. E. Shigley, *Gem. Gemology* **37**, 174 (2001).
24. J. E. Katon, *Micron* **27**, 303 (1996).